Closures Used in Zonally Averaged Ocean Models

DANIEL G. WRIGHT

Fisheries and Oceans Canada, Bedford Institute of Oceanography, Dartmouth, Nova Scotia, Canada

THOMAS F. STOCKER

Climate and Environmental Physics, Physics Institute, University of Bern, Bern, Switzerland

DOUGLAS MERCER

Department of Physics, Dalhousie University, Halifax, Nova Scotia, Canada

(Manuscript received 27 January 1997, in final form 23 July 1997)

ABSTRACT

There are at least three substantially different closures presently being used in two-dimensional ocean models. The main purpose of this paper is to clarify the assumptions that are implicit in these closures. Two of these formulations arise from zonally averaging the momentum equations: one has viscous damping represented by Fickian diffusion and the other by Rayleigh damping. Here a single equation is derived that includes both of these as special cases. The derivation shows that the Rayleigh damping term corresponds to horizontal diffusion of momentum into the western boundary and that this term is dominant for realistic parameter values. The vertical diffusion term can be neglected provided the Ekman transport is included in the surface layer, and the meridional diffusion term can be neglected if length scales less than 500 km are not resolved. If shorter length scales are considered, then the meridional diffusion term is required to avoid a numerical instability.

The third zonally averaged model formulation is based on vorticity dynamics. This approach has the advantage that the large geostrophic terms are eliminated by cross-differentiation so that attention is focused on the important ageostrophic effects. Previous work has shown that this formulation results in an improved fit to general circulation model results, but this fit depends on the use of a boundary condition that is somewhat ad hoc. Here the authors present a derivation that suggests a consistent dynamical interpretation of this boundary condition.

1. Introduction

Over the past several years, analyses of paleoclimate data have strongly suggested connections between climate change and changes in the large-scale ocean circulation. Furthermore, theoretical and numerical studies support the contention that changes in the global-scale oceanic overturning circulation may play an essential role in climate change. Unfortunately, the combination of long timescales, the need for multiple runs, and the computational expense of running coupled ocean–atmosphere models make the examination of oceanic influences on the climate system a time- and resource-consuming task. It is primarily for this reason that there has been a growing interest in low-order climate models that include credible representations of the oceans and their interaction with the atmosphere. Such models can also be coupled to bio–geochemical models that permit investigation of these processes over timescales previously inaccessible by three-dimensional models.

Low-order models of the ocean have been used to study climate-related issues for some time now. Using a simple box model, Stommel (1961) demonstrated the possibility that more than one ocean equilibrium may exist for identical forcing conditions and noted the potential significance to studies of the climate system. An important simplifying assumption in Stommel's model is that the zonally averaged flow moves down the meridional pressure gradient. Stommel makes it clear that his Rayleigh damped model is not expected to yield a very realistic representation of the real ocean circulation, but it has nevertheless resulted in important insights into the dynamical nature of the global-scale ocean circulation.

Marotzke et al. (1988, henceforth MWW) have used an alternative two-dimensional representation of the ocean circulation in which the meridional pressure gradient is balanced against Fickian vertical diffusion acting on the meridional overturning circulation. In the spirit of Stommel (1961), MWW present their model as an idealization of the real ocean, which is not dynam-

Corresponding author address: Dr. Daniel G. Wright, Ocean Science Division, P.O. 1006, Department of Fisheries and Oceans, Bedford Institute of Oceanography, Dartmouth, NS B2Y 4A2, Canada.
E-mail: dwright@emerald.bio.dfo.ca

ically accurate but nevertheless gives further insights into the nature and stability of the global thermohaline circulation.

Wright and Stocker (1991, henceforth WS) derive a zonally averaged ocean model based on the assumption that the zonally averaged zonal flow is similar to, but slightly reduced in magnitude in comparison with, the zonal average of the geostrophic component of the zonal flow. They point out that the resulting model is mathematically equivalent to a Rayleigh damped model and is hence consistent with the parameterization used by Stommel (1961), Rooth (1982), and Welander (1986). Stocker and Wright (1991) and Wright and Stocker (1992) generalize the model to include multiple basins and demonstrate somewhat surprisingly good agreement between model results and observed zonally averaged water mass properties, observational estimates of the meridional overturning circulation, and the stability of the overturning circulation found in more complete and computationally expensive 3D general circulation models.

Sakai and Peltier (1995, henceforth SP) have developed a 2D ocean circulation model that is dynamically similar to that used by MWW except that they include meridional diffusion of momentum and nonhydrostatic effects. Their results indicate that the nonhydrostatic effects cause no qualitative changes and even the quantitative changes are relatively small in comparison to those associated with changes in uncertain model parameters. Thus, the major difference from the MWW model is the inclusion of the meridional diffusion of momentum. The same approach was taken by Quon and Ghil (1996) and Saravanan and McWilliams (1995). Subsequently, SP follow the approach of Stocker and Wright (1991) to develop a model of the global ocean circulation by coupling 2D representations of the Pacific, Atlantic, and Indian Oceans through a representation of the Southern Ocean and reexamine the results of their previous study in this extended formulation.

A third zonally averaged model formulation for a single basin was introduced by Wright et al. (1995, henceforth WVH) and extended to a global geometry by Stocker and Wright (1996). This model formulation differs substantially from the earlier two in that it is the only one based on a set of well-defined physical assumptions about vorticity conservation and dissipation, and it is carefully compared with an extensive set of ocean general circulation model (OGCM) results.

Thus, there are now three substantially different zonally averaged model formulations, each of which has proven to provide useful insights into the role of the oceans in the climate system. Unfortunately, the connections between these different formulations have remained rather obscure. The primary purpose of the present paper is to clarify these connections. Based on considerations of the momentum equations, we derive a new closure scheme that includes each of the first two formulations discussed above as special cases. This approach makes it much easier to discern the relative merits of these approaches, and it more clearly reveals their common weaknesses.

The alternative assumptions and the results of the third approach are briefly reviewed. One weakness of the latter approach is that results depend on a somewhat uncertain specification of the boundary condition applied at the basin extremities. Additional support for this boundary condition is provided through a new physical interpretation.

2. Basic model equations

For the time and length scales of interest here, the ocean is effectively incompressible and the hydrostatic, Boussinesq, and rigid-lid approximations apply. For a non-eddy-resolving model, the inertial terms are also negligible. With these simplifications, the equations expressing the conservation of zonal, meridional, and vertical momentum; incompressibility; and conservation of heat and salt reduce to

$$-fv = -\frac{1}{\rho_* a\cos\phi}\frac{\partial p}{\partial \lambda} + \nabla_H\cdot(A_H\nabla_H u) + \frac{\partial}{\partial z}\left(A_V\frac{\partial u}{\partial z}\right) \quad (1)$$

$$fu = -\frac{1}{\rho_* a}\frac{\partial p}{\partial \phi} + \nabla_H\cdot(A_H\nabla_H v) + \frac{\partial}{\partial z}\left(A_V\frac{\partial v}{\partial z}\right) \quad (2)$$

$$\frac{\partial p}{\partial z} = -\rho_* g(1+\sigma) \quad (3)$$

$$\frac{1}{a\cos\phi}\frac{\partial u}{\partial \lambda} + \frac{1}{a\cos\phi}\frac{\partial(\cos\phi v)}{\partial \phi} + \frac{\partial w}{\partial z} = 0 \quad (4)$$

$$\frac{\partial T}{\partial t} + \frac{1}{a\cos\phi}\frac{\partial(uT)}{\partial \lambda} + \frac{1}{a\cos\phi}\frac{\partial(\cos\phi vT)}{\partial \phi} + \frac{\partial(wT)}{\partial z} = \nabla_H\cdot(K_H\nabla_H T) + \frac{\partial}{\partial z}\left(K_V\frac{\partial T}{\partial z}\right) + q_T^{\text{conv}} \quad (5)$$

$$\frac{\partial S}{\partial t} + \frac{1}{a\cos\phi}\frac{\partial(uS)}{\partial \lambda} + \frac{1}{a\cos\phi}\frac{\partial(\cos\phi vS)}{\partial \phi} + \frac{\partial(wS)}{\partial z} = \nabla_H\cdot(K_H\nabla_H S) + \frac{\partial}{\partial z}\left(K_V\frac{\partial S}{\partial z}\right) + q_S^{\text{conv}}, \quad (6)$$

where $\nabla_H(\ ) = \partial(\ )/(a\cos\phi\partial\lambda) + \partial(\ )/(a\partial\phi)$, λ, ϕ, and z are the longitude, latitude, and vertical coordinates, respectively, and u, v, w are the corresponding velocity components. Here z increases upward from the position of the sea surface at rest, T and S are temperature and salinity, p is pressure, $\rho(T, S, p)$ is the density calculated according to a simple, but fully nonlinear, equation of state (Wright 1997), and σ is the relative density difference $(\rho - \rho_*)/\rho_*$. Also, a is the earth's radius, g is the acceleration due to gravity, and $f/2 = \Omega\sin\phi$ is the local vertical component of the earth's rotation; A_H and A_V are horizontal and vertical eddy viscosities, K_H and K_V are horizontal and vertical eddy diffusivities, and q_T^{conv} and q_S^{conv} represent the effects of convection on T and S. The basic geometry and assumed boundary layers are illustrated in Fig. 1.

Sakai and Peltier state that nonhydrostatic effects omitted from (3) have a ''small but significant'' influence in their zonally averaged model. Since the nonhydrostatic effects considered by them are associated with the viscous damping terms and since their eddy viscosities are chosen to be extremely large ($A_H \sim 10^8$ m^2 s^{-1}, $A_V \sim 10^3$ m^2 s^{-1}), it is clear that these small effects would be negligible if more realistic damping terms were used. Of course, there is no guarantee that other nonhydrostatic effects do not have important consequences for the large-scale circulation in the real 3D world. However, the credible results obtained in previous 2D and 3D modeling studies (nearly all of which use vertical mixing schemes in conjunction with the hydrostatic approximation), plus the conclusions of Send and Marshall (1995) based on 3D numerical studies of convection, encourage us to proceed with the mixing scheme described in Wright and Stocker (1992). To avoid adding unwarranted complexity to our model, we make the hydrostatic approximation throughout the remainder of this discussion.

At solid boundaries, we require no normal flow, no slip, and no normal gradients for temperature and salinity. At the surface, the system is forced by fluxes of momentum, heat, and water vapor (or by a virtual salt flux under the rigid-lid approximation).

3. Zonal averaging of the momentum equations

In this section, our discussion will focus on the assumptions and approximations used in zonally averaging the horizontal momentum equations, since this is the primary source of differences between the most commonly used 2D model formulations.

It is convenient to introduce local variables x, y such that $dx = a\cos\phi\, d\lambda$, $dy = a\, d\phi$. In terms of these variables, the zonally averaged equations are

$$-f\overline{v} = -\frac{1}{\rho_*}\frac{\Delta p}{L} + \overline{(A_H u_x)_x} + \overline{(A_H u_y)_y} + \overline{(A_V u_z)_z}, \quad (7)$$

$$f\overline{u} = -\frac{1}{\rho_*}\frac{\partial\overline{p}}{\partial y} + \overline{(A_H v_x)_x} + \overline{(A_H v_y)_y} + \overline{(A_V v_z)_z}, \quad (8)$$

$$\frac{\partial\overline{p}}{\partial z} = -\rho_* g(1 + \overline{\sigma}), \quad (9)$$

$$\frac{1}{\cos\phi}\frac{\partial(\cos\phi\overline{v})}{\partial y} + \frac{\partial\overline{w}}{\partial z} = 0 \quad (10)$$

$$\frac{\partial\overline{T}}{\partial t} + \frac{1}{\cos\phi}\frac{\partial(\cos\phi\overline{v}\,\overline{T})}{\partial y} + \frac{\partial(\overline{w}\,\overline{T})}{\partial z} = \frac{\partial}{\partial y}\left(K_H\frac{\partial\overline{T}}{\partial y}\right) + \frac{\partial}{\partial z}\left(K_V\frac{\partial\overline{T}}{\partial z}\right) + q_T^{\text{conv}} \quad (11)$$

$$\frac{\partial\overline{S}}{\partial t} + \frac{1}{\cos\phi}\frac{\partial(\cos\phi\overline{v}\,\overline{S})}{\partial y} + \frac{\partial(\overline{w}\,\overline{S})}{\partial z} = \frac{\partial}{\partial y}\left(K_H\frac{\partial\overline{S}}{\partial y}\right) + \frac{\partial}{\partial z}\left(K_V\frac{\partial\overline{S}}{\partial z}\right) + q_S^{\text{conv}}, \quad (12)$$

where $L = a\cos\phi\Delta\Lambda$ is the width of the basin of angular extent $\Delta\Lambda$ and $\overline{(\ )} = (1/L)\int_{x_0}^{x_0+L}(\ )\, dx$ denotes a zonal average.

Some simplifications have been made in (7)–(12). First, in writing the diffusion terms, we have dropped terms that appear in spherical coordinates due to variations of the metrics on the planetary scale. Our horizontal diffusion terms will be assumed negligible except in boundary layers of width δ, so dropping these terms effectively neglects terms of order δ/a or smaller. Also, the contributions to the advection terms from the gyre circulation and zonal overturning are not explicitly represented; that is, we have used $\overline{vT} = \overline{v}\,\overline{T}$, $\overline{wT} = \overline{w}\,\overline{T}$, and similarly for salinity. In using these simplified expressions, we have neglected the stirring in the horizontal plane associated with the horizontal gyres and the stirring in the vertical plane associated with the zonal overturning circulation. Both K_H and K_V are to be increased as partial compensation. It is important to recognize that this approximation is either explicitly or implicitly made in all zonally averaged models. Any heat or salt fluxes associated with either horizontal gyre circulations or zonal overturning cells are represented by downgradient horizontal and vertical diffusion terms in the conservation equations. It is far from clear that these are good representations.

The above set of equations is the basic dynamical system that we wish to solve, but it does not contain enough information to determine either the zonally av-

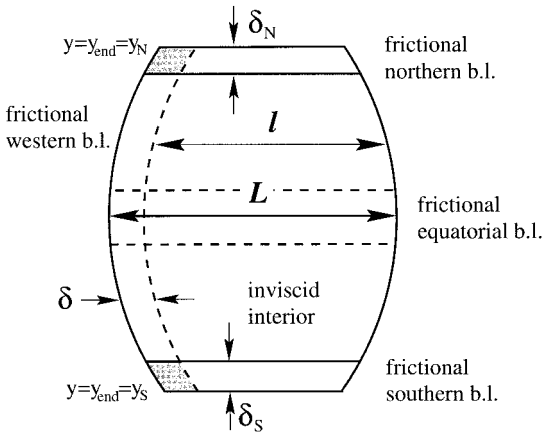

FIG. 1. The basic model geometry and boundary layer structures assumed in the text.

eraged dissipation terms or Δp, the zonal pressure difference across the basin. We now consider the approximations that are required in order to close this system of equations.

To begin, consider the term $\overline{(A_H v_x)_x}$, which allows for dissipation of momentum (and vorticity) in the western and/or eastern boundary layers. First, note that

$$\begin{aligned}\overline{(A_H v_x)_x} &= \frac{A_H}{L} v_x \Big|_{x_0}^{x_0+L} \\ &\approx -\frac{A_H}{L} v_x \Big|_{x_0} \\ &\approx -\frac{\gamma_1 A_H}{\delta L} \overline{v}^{\delta}, \end{aligned} \tag{13}$$

where an overbar alone indicates an average across the basin and a superscript, δ, indicates that the average is to be taken over just the western boundary layer. In the second line, consistent with observations, we have assumed that $A_H v_x|_{x_0+L} \ll A_H v_x|_{x_0}$, and in the third line we have approximated the horizontal shear at the inner edge of the western boundary in terms of the mean current across the boundary layer and the boundary layer width, δ. We will retain γ_1 as an undetermined factor, but the results of WVH show that if we approximate δ by the Munk boundary layer width $(A_H/\beta)^{1/3}$ (Munk 1950) then $\gamma_1 \approx 1$.

The quantity $\overline{v}^{\delta}$ must be represented in terms of some combination of $\overline{v}$ and the zonal average of the density. At least three different ways have been used to deal with this term:

1) Use the vorticity equation for the interior region (outside the western boundary layer) to determine the interior transport and then express the boundary layer transport as the difference between the total and the interior transport contributions (WVH)
2) Assume $\delta\overline{v}^{\delta} \propto L\overline{v}$ (WS)
3) Simply omit the term (SP).

Only the first approach is dynamically consistent. Results based on vorticity dynamics are discussed in detail by WVH and reviewed in the next section.

The second approach is implicitly used by Wright and Stocker (1991) and will be explicitly used here. If we consider a closed basin, then, based on the work of Stommel and Arons (1960a,b), we might take $\delta\overline{v}^{\delta} = 2L\overline{v}$. On the other hand, if we were to argue that the western boundary layer carries most of the transport, then we would use $\delta\overline{v}^{\delta} = L\overline{v}$. The differences between these two estimates reflect the uncertainty in using this approximation. In practice, the value of the proportionality factor has been chosen to give the best fit to OGCM results and observations.

The third approach completely neglects dissipation in the western boundary layer associated with horizontal diffusion. This approach is used by Sakai and Peltier (1995) [their Eq. (A6)]. The neglect of this term appears to have been an oversight. Unfortunately, it invalidates much of the discussion presented in their appendix A.

Diffentiating (13) and using the second of these approaches gives

$$\overline{(A_H v_x)_{xz}} = -\frac{\Gamma_1 A_H}{\delta^2} \overline{v}_z, \tag{14}$$

where Γ_1 may vary spatially but is of order unity. Note that dissipation in the western boundary layer is effectively represented by a Rayleigh damping term, $-\mu\overline{v}$, with $\mu = \Gamma_1 A_H/\delta^2$.

The next term that must be dealt with is the damping term associated with meridional gradients. Away from zonal boundary layers, this term will be negligible in comparison with the dissipation in the western boundary layer. To avoid unwarranted complications, we assume that A_H is zonally uniform and that variations in the basin width are negligible over the boundary layer scale δ. In this case, the averaging operator may be passed through the derivatives to yield an expression in terms of meridional gradients of $\overline{v}$; that is, if $L_y/L \ll \delta^{-1}$, then

$$\overline{(A_H v_y)_y} \approx (A_H \overline{v}_y)_y. \tag{15}$$

This approximation is consistent with the equations used by Fichefet and Hovine (1993) and Sakai and Peltier (1995).

Finally, we must deal with the appearance of $\overline{u}$ in the zonally averaged equations. This is where the most questionable compromises must be made in order to make further progress based on the momentum equations. We follow Wright and Stocker (1991), with some additional clarification. First we write

$$\frac{1}{\rho_*}\frac{\partial \overline{p}}{\partial y} + f\overline{u} = -f(\overline{u}_g - \overline{u}). \tag{16}$$

Substituting (14), (15), and (16) into (8) shows that the meridional overturning circulation [i.e., $(\overline{v}, \overline{w})$] is close-

ly associated with the small deviations from zonal geostrophy. Wright and Stocker (1991) assume that the quantity in parentheses is linearly related to $\overline{u}_g$ and then use OGCM results to estimate the magnitude of the constant of proportionality. It is of interest to estimate the magnitude of this quantity more directly, and this is done below.

First, we rewrite the difference between the zonal averages of the geostrophic flow and the total flow:

$$\overline{u}_g - \overline{u} = \frac{l(\overline{u}_g^I - \overline{u}^I) + \delta(\overline{u}_g^\delta - \overline{u}^\delta)}{L} = \frac{\delta}{L}\Gamma_2\overline{u}_g, \quad (17)$$

where

$$\Gamma_2 = \frac{\overline{u}_g^\delta - \overline{u}^\delta}{\overline{u}_g} = \frac{\overline{u}_g^\delta - \overline{u}^\delta}{\overline{u}_g^I}\left(1 + O\left(\frac{\delta}{L}\right)\right). \quad (18)$$

$l = L - \delta$ is the width of the interior region, and we have used $\overline{u}^I = \overline{u}_g^I$.

The value of Γ_2 is expected to be positive because $u = u_g$ at the offshore edge of the western boundary layer and u is required to go to zero at the coastal boundary while u_g is not. WVH make the approximation $u_g|_\delta = 2\overline{u}_g^I$ (as it would if u_g increased linearly from zero at the eastern boundary to its value at the outer edge of the western boundary layer). If we supplement this approximation with the assumptions that u_g remains constant across the boundary layer and u decreases linearly from u_g at the seaward edge of the boundary layer to zero at the solid boundary, then the ratio of $\overline{u}_g^\delta - \overline{u}^\delta$ to $\overline{u}_g^I$ is estimated to be 1. Sakai and Peltier also assume that the flow outside of the western boundary layer is in geostrophic balance. They then assume that u is identically zero in the western boundary layer and that u_g is uniform across the basin. These assumptions again give $\Gamma_2 = 1$. In reality, it is likely that the deviations from geostrophy within the boundary layer are much smaller than either of these estimates presuppose, so we expect that Γ_2 should actually be substantially less than 1. This will be quantified by fitting the model to OGCM data in the final section of this paper.

The above discussion suggests that Γ_2 is of order 1 or less, and it almost certainly varies substantially about its mean value. In practice, both WS and SP assume that Γ_2 is a constant: the assumption that Γ_1 and Γ_2 can be approximated by constants is probably the weakest link in the chain of arguments used in deriving a closure scheme for the zonally averaged equations directly from the momentum equations.

Whether or not Γ_1 and Γ_2 are assumed constant, we may now rewrite (8) as

$$A_H^*\overline{v}_{zyy} + A_V^*\overline{v}_{zzz} - \frac{\Gamma_1 A_H^*}{\delta^2}\overline{v}_z = -g\overline{\sigma}_y, \quad (19)$$

where $A_H^* = (A_H L)/(\Gamma_2\delta)$, $A_V^* = (A_V L)/(\Gamma_2\delta)$. The three terms on the left side of this equation allow for dissipation in zonal boundary layers, the surface and bottom Ekman layers, and the western boundary layer, respectively. While the assumption that Γ_2 is a constant is a weakness of the momentum approach, its consistent appearance as a divisor of either A_H or A_V raises the possibility that this approximation may not be much worse than the use of constant coefficients in the diffusion terms, an approximation that has been made in many previous studies with both zonally averaged models and 3D OGCMs.

Equation (19) includes the WS, MWW, and SP closures as special cases. The WS closure is obtained by neglecting meridional and vertical diffusion of momentum and identifying $\Gamma_1 A_H^*/\delta^2$ with Ω/ϵ [compare (19) with (23) in Wright and Stocker (1991)]. The MWW closure is obtained by neglecting the first and third terms on the left side and identifying A_V^* with their effective vertical viscosity. The SP closure is obtained by neglecting the third term on the left side and identifying A_H^* and A_V^* with their effective horizontal and vertical viscosity coefficients. Correspondence with the SP model also requires that the zonal component of vorticity ($\omega = w_y - v_z$) be approximated by $-v_z$, but this is accurate to order $\mathrm{Ro}(H/L)^2$, where Ro is the Rossby number U/fL (e.g., LeBlond and Mysak 1978). The zonally averaged models considered by Quon and Ghil (1996) and Saravanan and McWilliams (1995) also neglect the third term in (19) and are hence dynamically similar to the SP model.

It is noteworthy that the factor of L/δ appearing in the definitions of A_H^* and A_V^* is consistent with the corresponding factor appearing on the right side of (A9) in SP. In both our derivation and the derivation given in the appendix of SP, this factor arises because the pressure gradient outside of the western boundary layer is assumed to be balanced by the Coriolis force, whereas friction plays an important role within the boundary layer. Although the Coriolis force does not explicitly appear in (19), it actually balances the meridional pressure gradient to order δ/L. This fact is directly responsible for the amplification of the effective viscosity coefficients, A_H^* and A_V^*, appearing in (19) and is an important feature of both the WS and SP model formulations.

In addition to the amplification of the effective viscosity identified above, SP include another factor of L/δ [see their Eq. (A13)], which is included ''in order that the viscous model accord with the OGCM data.'' It is apparent from (19) that, if the third term is neglected, then the coefficient of the first term must actually be increased by order $(L/\delta)^2$ in order to maintain a realistic overturning circulation. The ad hoc increase in A_H^* introduced by SP is required in order to compensate for the unjustified neglect of dissipation associated with the horizontal flux of momentum into the sidewalls [i.e., the third term in (19)].

Finally, it is of interest to compare the relative mag-

nitudes of the vertical and horizontal dissipation terms. The ratio of the second and third terms in (19) is

$$\frac{A_V \overline{v}_{zz}}{\mu \overline{v}} \approx \frac{A_V}{A_H} \frac{\delta^2}{H_v^2}, \tag{20}$$

where H_v is the vertical scale for variations in v. Outside of Ekman layers, H_v is of order 500 m or greater and δ is of order 200 km or less. Appropriate values of A_V and A_H for use in coarse-resolution models are very uncertain. They are generally taken to be substantially larger than the corresponding diffusivities K_V and K_H, presumably to account for momentum transfers by unresolved pressure variations. Typical values used in OGCMs are of order 10^{-3} m^2 s^{-1} for A_V, and 2.5×10^5 m^2 s^{-1} for A_H (e.g., Hughes and Weaver 1994). Using these values gives a ratio of 0.000 64. Clearly, the only significant role of vertical viscosity in such models is in the Ekman layers, which we assume to be embedded within the surface cells of our model. Fortunately, the net Ekman flux is independent of the vertical eddy viscosity and may be specified as an additional flux carried by the surface layer. Dropping the vertical viscosity term, with the understanding that the Ekman flux is to be added to the surface layer, gives

$$A_H^* \overline{v}_{zyy} - \frac{\Gamma_1 A_H^*}{\delta^2} \overline{v}_z = -g \overline{\sigma}_y. \tag{21}$$

This simplification is important since the finite difference approximation to (21) gives rise to a tridiagonal system of equations, which may be very accurately and efficiently solved using routines such as TRIDAG from *Numerical Recipes* (Press et al. 1986). The validity of this approximation has been tested by integrating the full equation (19) and comparing the results to calculations based on (21). Differences are found to be negligible.

Questions of resolution

Based on numerical experiments with horizontal resolution increased to resolve scales of order 100 km or less, Sakai and Peltier (1995) note that

> . . . with fixed boundary conditions the nature of the time dependence of the circulation that is developed by the [WS] model may be an extremely strong function of horizontal resolution.

They also state that

> . . . [their] model is free of the undesirable numerical sensitivities that are unavoidable in WS91 type models.

Following Marotzke et al. (1988), Wright and Stocker (1991) assumed that zonal boundary layers are embedded within the northern, southern, and equatorial cells of the model. As such, the model was never intended to be used at the scales for which SP have found it to be inapplicable. Nevertheless, this issue has been investigated by Mercer (1996) using (19) and it seems worthwhile to summarize the results of that investigation.

Mercer (1996) did a series of numerical experiments at meridional resolutions of 10°, 5°, and 2° with (19) in the WS and SP limits. For the SP runs, $A_V^* = 10^3$ m^2 s^{-1} and for the WS runs $A_V^* = 0$ m^2 s^{-1} were used, consistent with previous studies. Through consideration of a broad range of A_H^*, he comes to the following conclusions.

- Both the WS model and the SP model suffer from numerical sensitivity at high horizontal resolution if the horizontal viscosity is reduced to zero. Both models suffer from large amplitude grid-scale ''noise'' when the resolution is reduced much below 500 km.
- The inclusion of the meridional viscous term with values of horizontal viscosity similar to those used by SP eliminates the sensitivity to grid resolution in both models. In fact, reducing A_H^* from the values of order 3×10^8 m^2 s^{-1} used by SP to 10^7 m^2 s^{-1} does not result in an instability. Results obtained with the WS formulation are not sensitive to variations in A_H^* within this range.
- The solutions obtained with lower resolution using the WS formulation reasonably replicate those obtained with finer resolution plus the values of meridional viscosity mentioned above. (This result may well be modified if small spatial scales are included in the surface forcing. However, it is unlikely that zonally averaged models are appropriate for the examination of the effects of such small scales.)

To determine what ''realistic'' values of A_H^* might be, we first note that for a Munk boundary layer width of 200 km, with $\beta = 2 \times 10^{-11}$ m^{-1} s^{-1}, the eddy viscosity A_H must be of order 1.6×10^5 m^2 s^{-1}. Thus, for a basin 5000 km wide the ''effective'' viscosity, A_H^*, would be of order $25 \times 1.6 \times 10^5$ m^2 s^{-1} $= 4 \times 10^6$ m^2 s^{-1}. This estimate assumes that $\Gamma_2 \approx 1$. However, in section 5 we will find that the best fit to OGCM results is obtained with $\Gamma_2 = 0.17$, and using this information increases our estimate of the effective value of horizontal viscosity to 2.4×10^7 m^2 s^{-1}. This value is still subject to substantial uncertainty, but it represents a useful benchmark against which to evaluate our results. Based on this estimate, values of A_H^* of order 10^7 m^2 s^{-1} seem reasonable. Values an order of magnitude larger, as used in viscously damped model formulations (Sakai and Peltier 1995; Saravanan and McWilliams 1995), are difficult to justify within the present framework.

Clearly, SP's statement that ''(their) model is free of the undesirable numerical sensitivities that are unavoidable in WS91 type models'' is inaccurate. Both models suffer from numerical sensitivity for low values of eddy viscosity and both models can avoid this sensitivity by including horizontal viscosity similar to that used by SP. For horizontal resolutions of 5° or greater (as seems

appropriate for these models), horizontal viscosity is not required in either model formulation.

Finally, Mercer (1996) also shows results of numerical experiments that support our earlier conclusion that the vertical damping term is consistently negligible compared to the horizontal damping terms for the viscosity coefficients typically used in these models.

4. Zonal averaging of the vorticity equation

The validity of the formulation developed in the previous section depends strongly on our ability to parameterize the quantity $f\overline{u}_a \equiv f(\overline{u} - \overline{u}_g)$ [Eq. (16)]. The approach of WS was to assume that this quantity is proportional to $\overline{u}_g$ and the basis for this has been further clarified above. Numerical experiments have shown that the results obtained with this formulation are not very sensitive to modest variations in the factor multiplying this term [e.g., multiplication or division of the right side of (21) by $\cos\phi$ has little effect on the model results]. Nevertheless, the dependence on $\overline{u}_a$ is disconcerting for two reasons. First, since the ageostrophic component of velocity depends on a small difference between two large quantities, there are obvious concerns about accuracy. Second, the resulting formula for $\delta\overline{v}^{\delta}$ depends entirely on the local density field, a fact which, for example, appears to conflict with the idea of a deep western boundary current with its source at high latitudes.

The approach of WVH avoids these difficulties by deriving a closure scheme based on vorticity dynamics. The first problem is avoided because the pressure gradient (i.e., the geostrophic component of the flow) is eliminated from the outset and the second problem never arises because nonlocal effects are included. On the other hand, the WVH approach requires appropriate boundary conditions at the basin extremities due to the nonlocal nature of the equations, and this introduces its own uncertainties.

In this section we give a brief outline of the approach taken by WVH, which focuses on the basic dynamical assumptions. We then give a physical interpretation for the high-latitude boundary condition introduced by WVH. The reader is referred to WVH for a detailed derivation of the model equations.

The central equations used by WVH are the averages across the western boundary layer and across the remainder of the ocean basin of the vertical component of the vorticity equation:

$$(f\delta\overline{v}^{\delta})_y = \rho_*^{-1}[p|_{\delta}]_y - A_H\zeta_x|_{x_0}, \tag{22}$$

$$(fl\overline{v}^{I})_y = -\rho_*^{-1}[p|_{\delta}]_y + (rL\overline{u} - r\delta\overline{u}^{\delta})_y, \tag{23}$$

where damping associated with meridional and vertical gradients has been represented by a Rayleigh damping term in the momentum equations [$\propto r(u, v)$], the notation $|_{\delta}$ indicates evaluation at the outer edge of the western boundary layer (i.e., at $x = x_0 + \delta$), and $\overline{(\cdot)}^{\delta}$, $\overline{(\cdot)}^{I}$ indicate averages over the western boundary layer and the interior region, respectively. Dissipation associated with zonal variations has been assumed to dominate within the western boundary layer and assumed negligible outside of it.

We note that

$$\rho_*^{-1}[p|_{\delta}]_y = -fu^{(n)}|_{\delta}\frac{\partial s}{\partial y}, \tag{24}$$

where $u^{(n)}$ is the velocity component normal to the outer edge of the western boundary layer and $fu^{(n)}\delta s$ is the flux of planetary vorticity out of the western boundary layer; so, Eq. (22) states that the flux of planetary vorticity into the western boundary layer is either dissipated by zonal diffusion into the boundary or balanced by a divergence of the planetary vorticity flux within the boundary layer. Similarly, Eq. (23) states that the flux of planetary vorticity into the basin interior is either dissipated by meridional diffusion associated with the Rayleigh damping term or balanced by a divergence of the planetary vorticity flux within the interior of the basin.

The unknown pressure terms may be eliminated from (22) and (23) by differentiating with respect to z, then using the hydrostatic relation together with $[\sigma|_{\delta}]_y \approx 2\overline{\sigma}_y$. The latter approximation follows from assuming that the meridional density gradient increases linearly from zero at the eastern boundary to the eastern edge of the western boundary layer. Finally, representing the dissipation in the western boundary layer by

$$-A_H\zeta_x|_{x_0} \approx -A_Hv_{xx}|_{x_0} \approx \frac{\gamma_0 A_H}{\delta^2}\overline{v}^{\delta}, \tag{25}$$

where γ_0 is of order unity, gives

$$(f\delta\overline{v}_z^{\delta})_y - \gamma_1\beta\delta\overline{v}_z^{\delta} = -2g\overline{\sigma}_y, \tag{26}$$

$$(fl\overline{v}_z^{I})_y = 2g\overline{\sigma}_y + (rL\overline{u}_z)_y, \tag{27}$$

where $\gamma_1 = \gamma_0(A_H/\beta\delta^3)$ ($\gamma_1 \equiv \gamma_0$ for a Munk layer). Equations (26) and (27) can be rewritten in the forms

$$(\delta\overline{v}_z^{\delta})_y + \frac{(1-\gamma_1)\beta}{f}\delta\overline{v}_z^{\delta} = -\frac{2g}{f}\overline{\sigma}_y, \tag{28}$$

$$\beta\overline{v}_z^{I} - f\overline{w}_{zz}^{I} = l^{-1}(rL\overline{u}_z)_y, \tag{29}$$

where we have used the vertical derivative of the continuity equation for the interior region in the form

$$-\frac{2g}{f}\overline{\sigma}_y + (l\overline{v}_z^{I})_y = -l\overline{w}_{zz}^{I} \tag{30}$$

to rewrite the second equation.

Equation (28) may be interpreted as a continuity equation for the western boundary layer in which the second term represents upwelling within the boundary layer and the right side represents exchange with the inviscid in-

terior. The right side of (29) represents dissipation in zonal boundary layers. Outside of these boundary layers, (29) expresses the classic Sverdrup balance for the interior. WVH show that the best fit to coarse-resolution OGCM results is obtained with $\gamma_1 \approx 1.1$, but that setting $\gamma_1 = 1.0$ has little effect on the zonally averaged model results. They also show that setting $r = 0$ has little effect. Equations (28) and (29) show that, if these choices are made (i.e., $\gamma_1 = 1.0$, $r = 0.0$), then the WVH model reduces to a western boundary layer that acts as a stack of leaky pipes exchanging fluid horizontally with a Sverdrup interior.

From the above interpretation, it is clear that the boundary conditions used by WVH play an important role in determining the overturning circulation. Below, we review and interpret these boundary conditions.

For the interior transport, we follow WVH and assume that all flow across the equator occurs within the western boundary layer and hence the interior transport vanishes at the equator. If (27) is then integrated from the equator to arbitrary y, we obtain

$$l\overline{v}^I_z = \frac{2g}{f}(\overline{\sigma} - \overline{\sigma}_{\text{eq}}) + \frac{r}{f}(L\overline{u}_z - L\overline{u}_z|_{\text{eq}}), \quad (31)$$

where the subscript ''eq'' indicates evaluation at the equator.

For the western boundary layer transport, it is more natural to specify conditions at the basin extremities. WVH were motivated by the results of Stommel and Arons (1960a) and Kawase (1987) to consider a boundary condition that allows for either horizontal or vertical recirculation at high latitudes. Hence, they used

$$\delta\overline{v}^{\delta}_z = \gamma_2 l\,\overline{v}^I_z \quad \text{at} \quad y = y_{\text{end}}, \quad (32)$$

where y_{end} is either the northern or southern extremity of the basin. Note that $\overline{v}^I_z$ is determined by (31), so Eq. (32) completes the determination of the integrated transport shear at $y = y_{\text{end}}$. Below, we will derive results for the northern extremity of the basin; results for a closed southern boundary are directly analogous.

As discussed by WVH, (32) determines both the horizontal recirculation and how much water downwells within the unresolved boundary layers, which are embedded in the northernmost and southernmost grid cells of the model. Here $\gamma_2 = -1$ would imply that the flow turns horizontally with no upwelling or downwelling associated with unresolved boundary layers. However, if $\gamma_2 \neq -1$, then a nonzero value of $l\,\overline{v}^I_z$ implies either upwelling or downwelling within these regions. WVH give support for this boundary condition by showing that it results in excellent agreement between the results of an OGCM and the zonally averaged formulation with $\gamma_2 = -0.6$.

The primary purpose of the remainder of this section is to present an interpretation of the boundary condition applied at high latitudes by WVH. The discussion is heuristic, and the assumptions are probably too restrictive to yield generally applicable results. Nevertheless, the argument leads to a boundary condition consistent with that adopted by WVH and provides a physical explanation for why this boundary condition might apply. An additional objective of this discussion is to emphasize the importance of vorticity constraints in the determination of deep-water formation at high latitudes.

We begin with the momentum equations for the zonal boundary layers. Within these layers, we make the usual linear, hydrostatic, and Boussinesq approximations. In addition, we assume that the dominant source of dissipation is associated with meridional gradients in the zonal velocity. Note that this assumption pertains to the zonal integral across the entire width of the basin. With these assumptions, the momentum equations on a local β plane reduce to

$$-fv = -\frac{1}{\rho_*}\frac{\partial p}{\partial x} + A_H\frac{\partial^2 u}{\partial y^2} \quad (33)$$

$$fu = -\frac{1}{\rho_*}\frac{\partial p}{\partial y}. \quad (34)$$

The Ekman flux is to be added separately to the surface layer and balanced by a barotropic return flow.

Cross-differentiating (33) and (34), integrating across the width of the basin, and assuming that variations in L are negligible through the boundary layer, we obtain

$$(fL\overline{v})_y = -(A_H L\overline{u}_y)_{yy}. \quad (35)$$

Integrating (35) meridionally across the boundary layer and neglecting gradients at the outer edge in comparison with gradients at the solid boundary gives

$$fL\overline{v}|_{y_{\text{end}}-\delta_N} = (A_H L\overline{u}_y)_y|_{y_{\text{end}}}, \quad (36)$$

where δ_N is the thickness of the northern boundary layer (Fig. 1).

Following the same ''finite difference'' approach used earlier to represent gradients in the western boundary layer, we have

$$fL\overline{v}|_{y_{\text{end}}-\delta_N} = -A_H L\frac{\overline{\overline{u}}^{\delta_N}}{\delta_N^2}, \quad (37)$$

where the double overbar represents an areal average over the entire northern boundary layer. Note that we have not included an undetermined coefficient multiplying the right side of this equation as we did in the representation of frictional dissipation in the western boundary layer. This coefficient has been absorbed into δ_N and the equivalence of the right sides of (36) and (37) is effectively taken as the definition of δ_N.

We must now relate $\overline{u}^{\delta_N}$ to $\overline{v}^{\delta}$ at the basin extremities. To make this connection we assume that the average value of u across the northern boundary layer at the outer edge of the western boundary layer is linearly related to the mean across both the basin width and the boundary layer; that is,

$$\delta_N\overline{u}^{\delta_N}\big|_{x=\delta} = 2\gamma_3\delta_N\overline{\overline{u}}^{\delta_N}. \quad (38)$$

If both v^I and vertical exchange within the northern boundary layer were zonally uniform, then u would increase linearly away from the eastern boundary and γ_3 would equal 1. We include γ_3 to allow for the possibility of zonal variations in v^I and vertical exchange within this boundary layer. If we also assume that vertical exchange within the northwestern corner (i.e., where the northern and western boundary layers overlap, Fig. 1) is either zero or linearly related to the inflow from the interior, then

$$\delta\overline{v}^{\delta} = \gamma_4\delta_N\overline{u}^{\delta_N}\big|_{x=\delta} = 2\gamma_3\gamma_4\delta_N\overline{\overline{u}}^{\delta_N}. \tag{39}$$

Substituting (39) into (37) gives

$$L\overline{v}|_{y_{\text{end}}-\delta_N} = -\frac{1}{2\gamma_3\gamma_4}\frac{A_H}{f\delta_N^2}\frac{L}{\delta_N}\delta\overline{v}^{\delta}. \tag{40}$$

Finally, using

$$L\overline{v} = l\,\overline{v}^I + \delta\overline{v}^{\delta}, \tag{41}$$

the relation (40) can be rewritten as

$$\delta\overline{v}^{\delta} = \gamma_2 l\,\overline{v}^I, \tag{42}$$

where

$$\gamma_2 = -\left[1 + \frac{1}{2\gamma_3\gamma_4}\frac{A_H L}{f\delta_N^3}\right]^{-1}. \tag{43}$$

Equation (42) is of the form used by WVH. Note that $-\gamma_2$ is the fraction of water entering the northern boundary layer from the inviscid interior, which turns horizontally; the remainder turns vertically.

WVH use OGCM results to determine a ''best estimate'' for γ_2 of -0.6. From (43) it is clear that this estimate implies a value for the quantity $(\gamma_3\gamma_4)^{1/3}\delta_N$, which we will refer to as the ''effective'' northern boundary layer width. Rearranging (43) we find that for $\gamma_2 = -0.6$, this width is given by $\delta_N^{\text{eff}} = (0.75A_HL/f)^{1/3}$. The OGCM used $A_H = 2.5 \times 10^5$ m^2 s^{-1}, and the Atlantic basin extended to 70°N with a width of 60°, while the Pacific basin extended to 59.5°N with a width of 120°. Using these values gives effective northern boundary layer widths of 146 and 216 km for the Atlantic and Pacific basins, respectively. In order to determine the actual boundary layer widths we would have to know the values of $\gamma_3\gamma_4$. This quantity is expected to be of order 1, but a precise value cannot be given. On the other hand, the estimate of δ_N only varies as the cube root of this quantity and hence is not very sensitive to it. Even if $\gamma_3\gamma_4 = 0.25$ (a fairly extreme value), our estimate of the actual boundary layer widths are only 60% greater than the effective boundary layer widths. Thus, it is clear that these boundary layers are embedded within a single cell of the coarse-resolution OGCM with its latitudinal grid cell size of approximately 390 km.

Based on the relative sizes of the implied boundary layer widths and the model grid size, it is clear that the boundary layers are not well resolved, and it is likely that the amount of high-latitude downwelling is affected by the large grid size of the OGCM. This is a concern for these models. Nevertheless, the general consistency noted above encourages us to believe that this idealized boundary condition represents the dynamics of the coarse-resolution OGCM's high-latitude boundary layer in a reasonable manner. Of course, there is no guarantee that this boundary condition would also fit the results of a finer-resolution OGCM with realistic bottom topography, but it appears to be a reasonable representation for use in low-order climate models.

For completeness, we now reproduce the formula for the total overturning transport derived by WVH. Evaluating (31) at $y = y_{\text{end}}$, substituting the result into (42), and using $r \ll f_{\text{end}}$ gives

$$\delta\overline{v}_z^{\delta}\big|_{y_{\text{end}}} = \gamma_2\frac{2g}{f_{\text{end}}}(\overline{\sigma}_{\text{end}} - \overline{\sigma}_{\text{eq}}). \tag{44}$$

Integrating (26) and using (44) now gives

$$\delta\overline{v}_z^{\delta} = \frac{2g}{f}\left[\gamma_2\left(\frac{f}{f_{\text{end}}}\right)^{\gamma_1}(\overline{\sigma}_{\text{end}} - \overline{\sigma}_{\text{eq}}) + |f|^{\gamma_1}\int_y^{y_{\text{end}}}|f|^{-\gamma_1}\overline{\sigma}_{\xi}\,d\xi\right], \tag{45}$$

and adding (45) and (31) gives the total overturning transport:

$$L\overline{v}_z = \frac{2g}{f}\left[(\overline{\sigma} - \overline{\sigma}_{\text{eq}}) + \gamma_2\left(\frac{f}{f_{\text{end}}}\right)^{\gamma_1}(\overline{\sigma}_{\text{end}} - \overline{\sigma}_{\text{eq}}) + |f|^{\gamma_1}\int_y^{y_{\text{end}}}|f|^{-\gamma_1}\overline{\sigma}_{\xi}\,d\xi\right] + \frac{r}{f}(L\overline{u}_z - L\overline{u}_z|_{\text{eq}}). \tag{46}$$

Finally, we return to (35) to give a physical interpretation for the high-latitude boundary condition. Equation (35) can be rewritten as

$$f\overline{w}_z = \beta\overline{v} + L^{-1}(A_H L\overline{u}_y)_{yy}. \tag{47}$$

The first term on the right side reflects that vertical velocities are required to conserve potential vorticity even in the inviscid interior. Vortex tube stretching (compression) associated with any additional downwelling will tend to generate cyclonic (anticyclonic) relative vorticity in the upper (lower) parts of the water column. Under our assumption of a quasi steady state for the momentum equations, this must be compensated by vorticity dissipation within the boundary layer, which, in our model, can only be supplied by a zonal flow in the boundary layer rubbing against the zonal boundary. Thus, as illustrated schematically in Fig. 2, this boundary condition states that downwelling within this boundary layer must be accompanied by zonal flow such that viscous dissipation counteracts the tendency to generate relative vorticity. This balance is consistent with the split between horizontal and vertical turning of

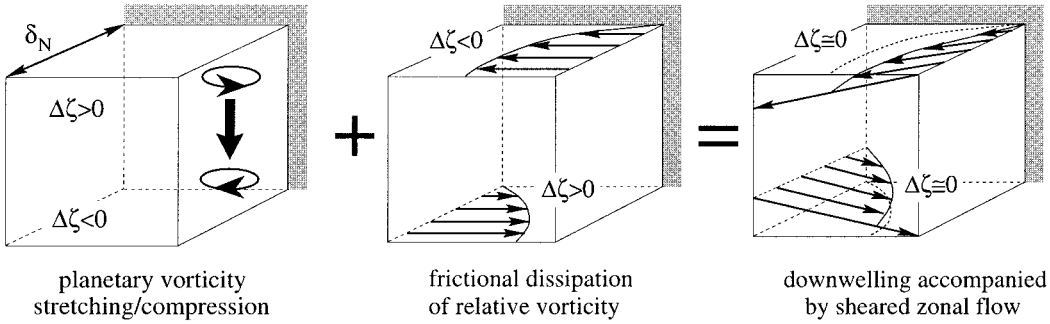

FIG. 2. Schematic illustration of the vorticity balance of the unresolved northern boundary layer of width δ_N. The left panel illustrates the effect of planetary vortex tube stretching, the middle panel indicates the opposing effect of frictional dissipation in zonal flows, and the right panel illustrates the combined effect of a balance between the vorticity generation by vortex tube stretching and frictionally induced vorticity dissipation.

the flow that enters the northern boundary layer from the inviscid interior of the OGCM.

5. Discussion and conclusions

The primary aim of this paper has been to clarify the assumptions that are implicitly made in the closures used in zonally averaged models. This was largely motivated by the fact that the assumptions implied by the two most commonly used closures, based on averaging the momentum equations, have not previously been systematically presented. For the closure based on the vorticity equation, a careful derivation of the zonally averaged equations has been given by WVH, and we have summarized the results briefly. However, we also provide a physical interpretation of the high-latitude boundary condition used by WVH, which was lacking from the original model formulation.

The basic results for the closures based on the momentum equations are encapsulated in (19). This equation includes the closures used by Marotzke et al. (1988), Sakai and Peltier (1995), and Wright and Stocker (1991) as special cases. The three closures differ in which of the terms on the left side are included: Wright and Stocker (1991) include only the third term, Marotzke et al. (1988) include only the second term, and Sakai and Peltier (1995) (also Quon and Ghil 1996 and Saravanan and McWilliams 1995) include the first and second terms.

Scale analysis of (19) indicates that the third term dominates. However, numerical experimentation shows that the first term is required to maintain stability if the meridional resolution is reduced much below 500 km. While consideration of such ''fine'' resolution was not contemplated in early studies, there may be cases in which the consideration of such scales is desirable. Fortunately, the second term is negligible in comparison with the third term except in the surface Ekman layer, and the influence of the Ekman transport can be accounted for by including this transport in the surface layer. This leads us to the simplified equation (21), which has the advantage that its finite difference representation yields a tridiagonal system of linear equations. This system may be solved with little more computational expense than required by the formulation of Wright and Stocker (1991) and substantially less computational expense than required by the formulation of Sakai and Peltier (1995). Further, the dynamical foundation of this equation is stronger than that used by Sakai and Peltier (1995) and it does not suffer from the resolution sensitivity found in either the Marotzke et al. (1988) or the Wright and Stocker (1991) formulations.

The dependence of the momentum approach formulation on the factor Γ_2, which remains uncertain, appears to be the major source of error for this case. The magnitude of Γ_2 is determined by the deviations from geostrophy in the western boundary layer. A primary advantage of the vorticity approach is that the pressure gradient is eliminated by cross-differentiating so one deals directly with the underlying vorticity balance rather than with small deviations from the degenerate geostrophic balance.

The main results regarding the vorticity closure scheme are encapsulated in (28), (29), and (43). The first two of these are equivalent to equations derived by WVH but rewritten in more readily interpreted forms. The first shows that the vorticity equation for the western boundary layer may also be interpreted as an integrated continuity equation. The second shows that outside of western and zonal boundary layers, the model dynamics reduces to a simple Sverdrup balance. Based on these equations, a useful limit of the WVH formulation ($\gamma_1 = 1$, $r = 0$) is seen to be consistent with a Sverdrup interior that exchanges fluid with the western boundary layer, which serves as a pipeline to other latitudes without any vertical exchange. The simplicity of this interpretation makes it attractive, but the dependence on the high-latitude boundary condition is somewhat disconcerting since the boundary condition used by WVH did not have a strong physical motivation.

Equation (43), and the derivation leading to it, represents a physical interpretation for this equation.

Downwelling in the northern boundary layer will cause vortex tube stretching in the upper part and vortex tube compression in the lower part of the water column, which will cause a positive vorticity tendency in the upper region and a negative tendency in the lower region. These tendencies must be balanced by viscous dissipation of vorticity and this is accomplished by the east–west flow within the boundary layer rubbing against the northern boundary (Fig. 2). Thus, stronger downwelling implies stronger westward (eastward) flow in the upper (lower) part of the water column in order to balance the vorticity tendencies. This balance gives the boundary condition used by WVH. It should be noted that we do not claim that this boundary condition will apply to more realistic situations (e.g., with realistic bottom topography or eddy-permitting resolution). However, this physical interpretation does emphasize the importance of vorticity constraints in determining the production of deep water, and this basic point does not depend on the simple model considered here. Further investigation of the controls on deep-water formation in more realistic situations is clearly warranted.

WVH show fits to OGCM results obtained with the WS and the WVH formulations that support the contention that the vorticity approach yields superior results to the approach of Wright and Stocker (1991). Their results are based on the zonally integrated meridional velocity component and the zonally averaged density from the eight NOWIND runs described by Hughes and Weaver (1994). The geometry consists of two basins representing the Pacific and Atlantic, connected by a circumpolar ocean. The Pacific is 120° wide and extends to 59.5°N, and the Atlantic is 60° wide and extends to 70°N. Horizontal and vertical eddy diffusion coefficients were $A_{TH} = 2 \times 10^3$ m^2 s^{-1} and $A_{TV} = 1.39 \times 10^{-4} + 0.78 \times 10^{-4} \tan^{-1}[5 \times 10^{-3} (-z - 1000)]$ m^2 s^{-1}. The corresponding momentum diffusion coefficients were $A_{MH} = 2.5 \times 10^5$ m^2 s^{-1} and $A_{MV} = 10^{-3}$ m^2 s^{-1}. The Bryan–Cox model was used for the integrations with a coarse resolution of 3.75° longitudinally, 3.5° latitudinally, and 19 levels in the vertical. The overturning circulations varied dramatically between the different runs: the maximum overturning in the Atlantic varied between 5 and 34×10^6 m^3 s^{-1}, while that in the Pacific varied between 0 and 33×10^6 m^3 s^{-1}.

Figure 3a illustrates the ability of (19), the generalized formula based on averaging the momentum equations, to represent the OGCM results. The quantity plotted corresponds to an integral from a depth of 130 m down to each of the cell boundaries of the OGCM. The model was fit to the OGCM results by dividing each of the terms in (19) by $\Gamma_1 A_H^*/\delta^2 L$, and then using linear regression to express the third term on the left side in terms of a linear combination of the remaining terms, in order to estimate the factors Γ_1 and Γ_2. Two problems arise in attempting to determine the coefficients of the diffusion terms based on the OGCM results. First, it is found that the OGCM results do not adequately constrain the value of the coefficient multiplying the vertical diffusion term (by taking different subsets of the OGCM ''data,'' the value can be anything between -20 and $+20$). This is as expected since the surface Ekman layer is not resolved by the model output. Because of this, the vertical diffusion term can be dropped entirely without affecting our results. The fit shown in Fig. 3a actually corresponds to (21) rather than (19). The second problem is that, when information within about 10° of the equator is included in the fitting procedure, the estimate of the coefficient multiplying the horizontal diffusion term becomes large and negative without significantly improving the fit to the data. This is probably a consequence of attempting to fit an inappropriate dynamical model to the equatorial region. For this reason, only the OGCM data outside of 10° from the equator are used in the fitting procedure. High-latitude data are included since the boundary layer information is required to constrain the coefficient of the horizontal diffusion term.

With the above restrictions, we find that the best fit of (21) to the OGCM data implies $\Gamma_1 = 0.83$ and $\Gamma_2 = 0.17$. Dropping the horizontal diffusion term entirely does not significantly affect the model fit, and the values of both Γ_1 and Γ_2 are not sensitive to how the data are subsampled, so the values of both coefficients appear to be well determined. It is noteworthy that the value of Γ_2 is consistent with the zonal flow being primarily geostrophically balanced, even within the western boundary layer.

Figure 3b shows the corresponding results of fitting Eq. (46), based on averaging the vorticity equation, to the same OGCM results. The fitting procedure is essentially the same as that used in WVH except that here we have avoided the complications associated with the nonlinear dependence on γ_1 by setting this parameter to the optimal value of 1.1 determined by WVH (using 1.0 or 1.2 does not substantially change our results). Thus, only the parameters γ_2 and r are determined here. Also, since zonal boundary layers are crudely accounted for through the Rayleigh coefficient, r, we have again included all of the OGCM data outside of 10° from the equator in the fitting procedure. This modification does not affect the estimate of γ_2, but it does have a modest affect on the estimate of r. Our optimal estimates of these parameters are $\gamma_2 = -0.6$ and $r = 2.2 \times 10^{-6}$ s^{-1}, which are not very different from the estimates of $\gamma_2 = -0.6$ and $r = 2.6 \times 10^{-6}$ s^{-1} obtained by WVH. We have also tried replacing the Rayleigh damping in the vorticity formulation with a horizontal Fickian diffusion term and found that this did not improve our results.

The main results illustrated by Fig. 3 are immediately obvious. First, the inclusion of Fickian diffusion terms in the WS formulation does not significantly improve our ability to represent OGCM results, which is consistent with the fact that dissipation in the western boundary layer dominates over dissipation in zonal or

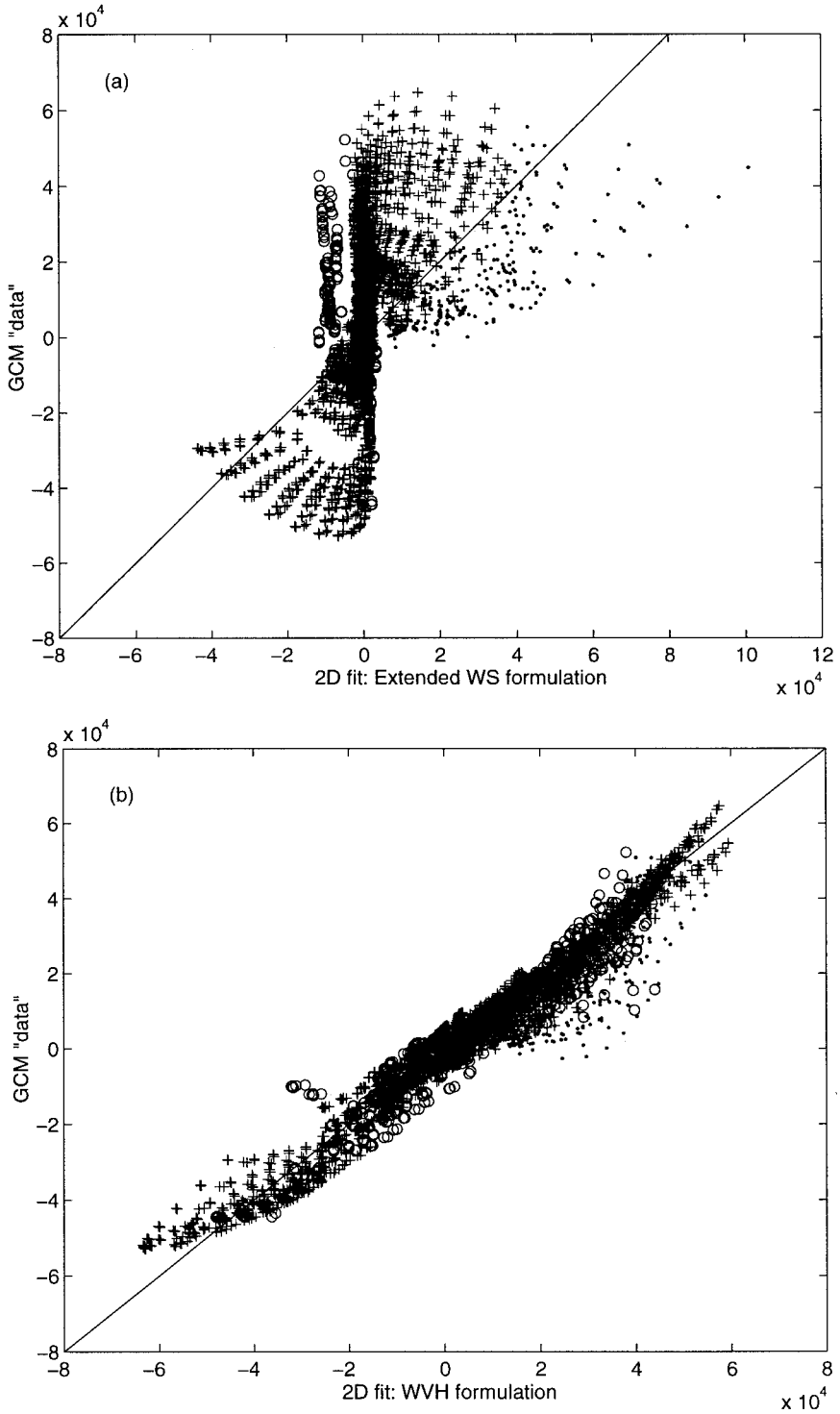

FIG. 3. (a) The 2D model fit to 3D OGCM data corresponding to (21). The quantity plotted is the difference in basin width times velocity between each model depth and 130 m in units of $m^2 s^{-1}$. Results within 10° of the equator are plotted as open circles and those within 10° of the northern boundaries are plotted as dots. (b) The corresponding fits based on (46).

vertical boundary layers. Second, the solution based on the vorticity approach represents the OGCM results far better than the solution based on the momentum approach.

In spite of the apparent superiority of the vorticity approach, the momentum approach remains of interest because it is easier to implement and does not suffer from resolution sensitivity at ''fine'' resolution, provided the meridional viscous term is included. Further, that the vertical momentum diffusion term can be neglected, if the Ekman flux is included in the surface layer, should not be interpreted to imply that the results of Marotzke et al. (1988), Sakai and Peltier (1995), or Saravanan and McWilliams (1995) are without value. In these models, the magnitude of the vertical friction term has been increased so as to crudely allow for the effect of horizontal diffusion into the western boundary and yield a reasonable overturning circulation. Our results suggest that a Rayleigh damping term is better suited to represent this effect, but the representation by the Fickian diffusion term should (and does) give a reasonable ''broad brush'' picture of the overturning circulation.

Finally, we note that the discussion presented here has focused on the momentum and vorticity equations and very little mention has been made of the approximations made in the tracer equations. In these equations, any meridional (vertical) mixing associated with horizontal gyres (zonal overturning) is assumed to be represented by an enhancement of the horizontal (vertical) diffusion term. In addition, tracer transports associated with smaller-scale eddies are also assumed to be represented by enhanced diffusion terms. These closures and the lack zonal structure in the forcing terms are probably the real limiting factors in models that use either the momentum or vorticity closures discussed here.

The role of the eddy-induced tracer transports has been emphasized by Gent and McWilliams (1990) and Gent et al. (1995). The addition of these effects leaves the basic results obtained with coarse-resolution OGCMs unchanged, so one might wonder if these ''higher-order'' effects are worth considering in the ''lower-order'' representations obtained with 2D models. Preliminary tests indicate that inclusion of these terms in the WVH formulation does result in significant improvements, primarily in the Southern Ocean.

Gent et al. (1995) point out that, when the momentum equations are cast in terms of the tracer transport velocity (including the mean velocity and the diapycnal component of the eddy-induced transport velocity), the closure proposed by Gent and McWilliams (1990) can be expressed as a vertical transfer of momentum with an effective vertical viscosity of order $(f/N)^2\kappa$, where κ is of order 10^3 m^2 s^{-1}. This observation has been used by Saravanan and McWilliams (1995) as partial justification for the large value of vertical viscosity required in their model. However, as they note, the vertical viscosity that they use is ''probably somewhat too large to be realistic,'' and even with this large damping term, the overturning circulation remains too large. We believe that this is a consequence of neglecting the viscous damping associated with the western boundary layer [the third term in (19)].

In our discussion we have taken our velocities to represent time mean values (excluding the eddy transports) with the understanding that all eddy effects must be accounted for in the tracer equations. If the momentum equations are recast in terms of the tracer transport velocities, the vertical diffusion term in (19) must be retained and the viscosity coefficient should be passed through two of the vertical derivatives and allowed to vary with both latitude and vertical stratification.

Acknowledgments. This study was supported by the Canadian Natural Sciences and Engineering Research Council through the Climate System History and Dynamics Project and by the Swiss National Science Foundation. TFS is grateful for the hospitality extended by A. Clarke and T. Bowen during a visit to Bedford Institute and Dalhousie University in August 1996.

REFERENCES

Bryan, F., 1987: Parameter sensitivity of primitive equation ocean general circulation models. *J. Phys. Oceanogr.,* **17,** 970–985.

Bryan, K., and L. J. Lewis, 1979: A water mass model of the world ocean. *J. Geophys. Res.,* **84,** 2503–2517.

Cox, M. D., 1985: An eddy resolving numerical model of the ventilated thermocline. *J. Phys. Oceanogr.,* **15,** 1312–1324.

Fichefet, T., and S. Hovine, 1993: The glacial ocean: A study with a zonally averaged, three-basin ocean circulation model. *Ice in the Climate System,* W. R. Peltier, Ed., NATO ASI Series, Vol. I 12, Springer-Verlag, 433–458.

Gent, P. R., and J. C. McWilliams, 1990: Isopycnal mixing in ocean circulation models. *J. Phys. Oceanogr.,* **20,** 150–155.

——, J. Willebrand, T. J. McDougall, and J. C. McWilliams, 1995: Parameterizing eddy-induced tracer transports in ocean circulation models. *J. Phys. Oceanogr.,* **25,** 463–474.

Hughes, T. M. C., and A. J. Weaver, 1994: Multiple equilibria of an asymmetric two-basin ocean model. *J. Phys. Oceanogr.,* **24,** 619–637.

Kawase, M., 1987: Establishment of deep ocean circulation driven by deep water production. *J. Phys. Oceanogr.,* **17,** 2294–2317.

LeBlond, P. H., and L. A. Mysak, 1988: *Waves in the Ocean.* Elsevier, 602 pp.

Marotzke, J., P. Welander, and J. Willebrand, 1988: Instability and multiple equilibria in a meridional-plane model of the thermohaline circulation. *Tellus,* **40A,** 162–172.

Mercer, D., 1996: Atmospheric water vapour transport and the thermohaline circulation. M.S. thesis, Department of Physics, Dalhousie University, 177 pp. [Available from Dept. of Physics, Dalhousie University, Halifax, NS B2Y 4AZ, Canada.]

Munk, W. H., 1950: On the wind driven ocean circulation. *J. Meteor.,* **7,** 79–93.

Press, W. H., B. P. Flannery, S. A. Teukolsky, and W. T. Vetterling, 1986: *Numerical Recipes: The Art of Scientific Computing.* 2d ed. Cambridge University Press, 963 pp.

Quon, C., and M. Ghil, 1996: Multiple equilibria in thermosolutal convection due to salt-flux boundary conditions. *J. Fluid Mech.,* **245,** 449–483.

Rooth, C., 1982: Hydrology and ocean circulation. *Progress in Oceanography,* Vol. 11, Pergamon, 131–149.

Sakai, K., and W. R. Peltier, 1995: A simple model of the Atlantic

thermohaline circulation: Internal and forced variability with paleoclimatological implications. *J. Geophys. Res.,* **100,** 13 455–13 479.

——, and ——, 1996: A multibasin reduced model of the global thermohaline circulation: Paleoceanographic analyses of the origins of ice-age climate variability. *J. Geophys. Res.,* **101,** 22 535–22 562.

Saravanan, R., and J. C. McWilliams, 1995: Multiple equilibria, natural variability, and climate transitions in an idealized ocean–atmosphere model. *J. Climate,* **8,** 2296–2323.

Send, U., and J. Marshall, 1995: Integral effects of deep convection. *J. Phys. Oceanogr.,* **25,** 855–872.

Stocker, T. F., and D. G. Wright, 1991: A zonally averaged model for the thermohaline circulation. Part II: Interocean exchanges in the Pacific–Atlantic basin system. *J. Phys. Oceanogr.,* **21,** 1725–1739.

——, and ——, 1996: Rapid changes in ocean circulation and atmospheric radiocarbon. *Paleoceanography,* **11,** 773–796.

Stommel, H., 1961: Thermohaline convection with two stable regimes of flow. *Tellus,* **13,** 224–241.

——, and A. B. Arons, 1960a: On the abyssal circulation of the world ocean—I. Stationary planetary flow patterns on a sphere. *Deep-Sea Res.,* **6,** 140–154.

——, and ——, 1960b: On the abyssal circulation of the world ocean—II. An idealized model of the circulation pattern and amplitude in oceanic basins. *Deep-Sea Res.,* **6,** 217–233.

Welander, P., 1986: Thermohaline effects in the ocean circulation and related simple models. *Large-Scale Transport Processes in Oceans and Atmosphere,* J. Willebrand and D. L. T. Anderson, Eds., D. Reidel, 163–200.

Wright, D. G., 1997: An equation of state for use in ocean models: Eckart's formula revisited. *J. Atmos. Oceanic Technol.,* **14,** 735–740.

——, and T. F. Stocker, 1991: A zonally averaged ocean model for the thermohaline circulation. Part I: Model development and flow dynamics. *J. Phys. Oceanogr.,* **21,** 1713–1724.

——, and ——, 1992: Sensitivities of a zonally averaged global ocean circulation model. *J. Geophys. Res.,* **97,** 12 707–12 730.

——, C. B. Vreugdenhil, and T. M. Hughes, 1995: Vorticity dynamics and zonally averaged ocean circulation models. *J. Phys. Oceanogr.,* **25,** 2141–2154.